Role of furin in granular acidification in the endocrine pancreas: Identification of the V-ATPase subunit Ac45 as a candidate substrate

Els Louagie*, Neil A. Taylor*†, Daisy Flamez‡, Anton J. M. Roebroek*, Nicholas A. Bright§, Sandra Meulemans*, Roel Quintens¶, Pedro L. Herrera‖, Frans Schuit¶, Wim J. M. Van de Ven*, and John W. M. Creemers*,**

Departments of *Human Genetics, Box 602, and ¶Molecular Cell Biology, Katholieke Universiteit Leuven, Gasthuisberg O/N 1, Herestraat 49, B-3000 Leuven, Belgium; †Cancer Research UK, Cambridge Research Institute, Li Ka Shing Centre, Robinson Way, Cambridge CB2 0RE, United Kingdom; ‡Laboratory of Experimental Medicine, Université Libre de Bruxelles, Route de Lennik 808, B-1070 Brussels, Belgium; §Cambridge Institute for Medical Research, University of Cambridge, Addenbrooke's Hospital, Hills Road, Cambridge CB2 0XY, United Kingdom; and ‖Department of Genetic Medicine and Development, Faculty of Medicine, University of Geneva, Rue Michel-Servet 1, CH-1211 Geneva 4, Switzerland

Edited by Donald F. Steiner, University of Chicago, Chicago, IL, and approved June 16, 2008 (received for review January 12, 2008)

Furin is a proprotein convertase which activates a variety of regulatory proteins in the constitutive exocytic and endocytic pathway. The effect of genetic ablation of *fur* was studied in the endocrine pancreas to define its physiological function in the regulated secretory pathway. *Pdx1-Cre*/loxP furin KO mice show decreased secretion of insulin and impaired processing of known PC2 substrates like proPC2 and proinsulin II. Both secretion and PC2 activity depend on granule acidification, which was demonstrated to be significantly decreased in furin-deficient β cells by using the acidotrophic agent 3-(2,4-dinitroanilino)-3′amino-*N*-methyldipropylamine (DAMP). Ac45, an accessory subunit of the proton pump V-ATPase, was investigated as a candidate substrate. Ac45 is highly expressed in islets of Langerhans and furin was able to cleave Ac45 *ex vivo*. Furthermore, the exact cleavage site was determined. In addition, reduced regulated secretion and proinsulin II processing could be obtained in the insulinoma cell line βTC3 by downregulation of either furin or Ac45. Together, these data establish an important role for furin in regulated secretion, particularly in intragranular acidification most likely due to impaired processing of Ac45.

endoprotease | insulin | islets of Langerhans | proton pump | proprotein convertase

Proprotein convertases (PCs) are a family of seven closely related subtilisin-like serine endoproteases [furin, PC1/3, PC2, PC4, PC5/6, paired basic amino acid converting enzyme 4 (PACE4), and PC7] (1) and two more distantly related members subtilisin/kexin-like isozyme-1/site-1 protease (SKI-1/S1P) and neural apoptosis regulated convertase-1/proprotein convertase subtilisin/kexin type 9 (NARC-1/PCSK9) (2). Although many potential *in vivo* substrates have been identified based on *in vitro* and *ex vivo* analysis, data obtained from KO mice and human patients have highlighted the limitations of the studies (1, 3, 4).

The KO mouse model of the ubiquitously expressed convertase furin is early embryonically lethal, indicating vital, nonredundant functions of this enzyme at early developmental stages (5). However, this embryonic lethality precludes the analysis of many substrates expressed only in adult stage or well differentiated tissues. Therefore, a conditional KO mouse model has been generated (6). Remarkably, an inducible furin KO mouse model, in which near complete inactivation of the *fur* (*Fes Upstream Region*; GenBank accession no. 18550) gene was obtained in liver, showed no detectable histological defects. Variable degrees of redundancy were observed for the processing of candidate substrates. This redundancy is probably because of the expression of PACE4, PC5/6, and PC7 in the constitutive secretory pathway of the liver.

Contrary to the liver, the endocrine pancreas contains a constitutive as well as a regulated secretory pathway. Because furin has been shown to control proliferation as well as differentiation of pancreatic β cell lines (7), we focused on the *in vivo* role of furin in the endocrine pancreas to define its possible physiological function in the regulated secretory pathway.

Intracellularly furin is known to be concentrated in the *trans*-Golgi network (TGN), although ImmunoGold electron microscopy also revealed the presence of small amounts of furin on the periphery of immature secretory granules (ISG) (8). Furin is excluded from the mature secretory granules through phosphorylation of its cytoplasmic domain by casein kinase II and subsequent interaction with adaptor protein (AP)-1, a component of the TGN/ISG-localized clathrin sorting machinery (9). However, a function of furin in ISG is not yet known.

In contrast, the role of PC1/3 and PC2 in the regulated secretory pathway is well established (10). In pancreatic β cells, processing of proinsulin into mature insulin requires cleavage by PC1/3 and PC2, C-terminal of paired basic residues that are subsequently removed by carboxypeptidase E (CPE) (11). Autocatalytical cleavage of the propeptide of proPC1/3 occurs rapidly after biosynthesis (12). After a slow folding process, proPC2 is not converted in the endoplasmic reticulum (ER), but is as such transported to TGN and ISG. Its chaperone pro7B2 increases proPC2 transport through stabilization (13). The low pH and high calcium concentration of these late secretory compartments trigger the conversion of proPC2 to mature PC2 (14). This mature PC2 is activated only when pro7B2 is cleaved by a furin-like protease in the TGN (15).

Acidification of the secretory granules is not only necessary for PC1/3 and PC2 activity and hence proprotein processing (16) but also for priming of the granules at the plasma membrane, a prerequisite for secretion (17). Various organelles are acidified through a proton gradient, established and maintained by the H^+-pumping vacuolar-type ATPase (V-ATPase). This multisubunit enzyme can be differentially regulated in those intracellular compartments (18). Of interest to this research, a mutation in *KEX2* (killer expression 2; encoding the yeast ortholog of furin) in *Saccharomyces cerevisiae*, was found to exert an inhibitory effect on V-ATPase activity (19).

Author contributions: F.S., W.J.M.V.d.V., and J.W.M.C. designed research; E.L., N.A.T., D.F., N.A.B., S.M., and R.Q. performed research; A.J.M.R. and P.L.H. contributed new reagents/analytic tools; E.L., N.A.T., D.F., and R.Q. analyzed data; and E.L., N.A.T., and J.W.M.C. wrote the paper.

The authors declare no conflict of interest.

This article is a PNAS Direct Submission.

**To whom correspondence should be addressed. E-mail: john.creemers@med.kuleuven.be.

This article contains supporting information online at www.pnas.org/cgi/content/full/0800340105/DCSupplemental.

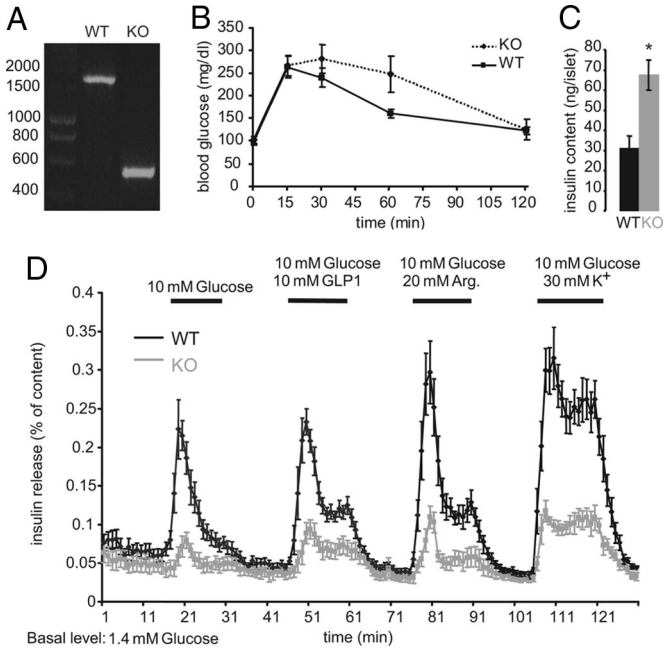

Fig. 1. Inactivation of furin in islets of Langerhans: reduced insulin release and increased insulin content. (*A*) PCR analysis of deletion of *fur* exon 2 in islets of Langerhans of $fur^{flox/flox}$ mice (WT) and $fur^{flox/flox}$, *Pdx1-Cre* mice (KO). Primers were designed to correspond to intronic sequences outside *fur* exon 2 and loxP sequences. DNA fragment sizes (bp) are indicated. (*B*) Glucose tolerance test on 2-month-old male mice. Mice were fasted overnight and i.p. injected with 1 mg/g of glucose at time point 0. Data represent mean values ± SEM, $n = 10$ mice per genotype. (*C*) Islet insulin content was extracted after the perifusion experiment (see *D*) and measured by using RIA. Data represent means ± SEM ($n = 4$ experiments). *, $P < 0.05$. (*D*) Islets of 2-month-old male mice were perifused 16 h after isolation. A 15-min preperifusion with basal medium containing 1.4 mM glucose was followed with a sequence of 15-min exposures to medium containing either 10 mM glucose alone or supplemented with 10 mM GLP1, 20 mM Arg, or 30 mM K^+. Data represent means ± SEM ($n = 4$ experiments).

In this article, we describe a mouse model for pancreas-specific genetic ablation of the *fur* gene. For this purpose, we crossed *Pdx1* (*pancreatic and duodenal homeobox factor 1*)-*Cre* transgenic mice (20) with the previously described conditional furin KO mice (6). The observed phenotype prompted us to investigate Ac45 (encoded by *Atp6ap1*, *H+ transporting*, *lysosomal accessory protein 1*; GenBank accession no. 54411), an accessory subunit of the V-ATPase, as candidate substrate.

Results

Inactivation of Furin in the Islets of Langerhans. Conditional inactivation of furin was achieved by crossing the previously described $fur^{flox/flox}$ mice, in which exon 2 of *fur* is flanked by loxP sites on both alleles, with *Pdx1-Cre* transgenic mice (6, 20). By using the promoter of *Pdx1*, the earliest marker of the developing pancreas, Cre recombinase is expressed in all pancreatic epithelial cell lineages. It has been established that subsequent deletion of exon 2 sequences, encoding the translation initiation site, the signal peptide, and part of the prodomain of furin, inactivates the *fur* gene (6). Offspring heterozygous for the floxed *fur* allele and the *Pdx1-Cre* transgene were intercrossed to obtain homozygous $fur^{flox/flox}$ mice carrying in addition one or two *Pdx1-Cre* alleles (referred to as KO). Cre recombination of the floxed *fur* alleles was confirmed on DNA of isolated islets of Langerhans (Fig. 1*A*). Deletion of the floxed exon 2 resulted in a PCR product, 1 kb smaller than without Cre recombinase activity. These pancreas-specific furin KO mice were born in Mendelian proportions and equal male/female ratio, and they showed normal growth and fertility.

Impaired Insulin Secretion by the Furin-Deficient Islets of Langerhans. Although the mice appeared healthy, slight differences in glucose tolerance were observed between KO ($fur^{flox/flox}$, *Pdx1-Cre*) and WT ($fur^{flox/flox}$) littermates (Fig. 1*B*). After glucose injection, the pancreas-specific KO mice tended to have higher blood glucose levels than WT mice after 60 min. However, this difference was not significant, because of large mouse-to-mouse differences in the KO mice. After 120 min, blood glucose concentrations were back to normal.

To investigate this mild glucose intolerance in more detail, insulin-release kinetics of isolated islets was analyzed in a dynamic perifusion system. A clearly reduced insulin release (in the first and second phase) by the KO islets was shown in response to glucose stimulation alone or together with glucagon-like peptide 1 (GLP1), potassium, and arginine (Fig. 1*D*). Insulin content was twice as high in furin-deficient islets, probably as a consequence of impaired secretion (Fig. 1*C*).

No significant difference was observed between WT and KO mice in the number of islets per pancreas [supporting information (SI) Fig. S1*A*] nor in the islet area compared with total pancreas area (Fig. S1*B*). Morphologically, the islets appeared normal, although an increased number of mislocalized α cells and δ cells within the β cell mass was observed (data not shown). At the ultrastructural level, no obvious differences were seen between WT and KO islets (Fig. S1 *C* and *D*).

Impaired Processing of Proproteins in the Furin-Deficient Islets of Langerhans. To obtain insight into the differences at the biochemical level, processing of neuroendocrine proproteins was analyzed. First, the conversion of the main β cell secretory product, proinsulin to insulin, was examined. Mouse proinsulin II can be selectively labeled with [^{35}S]methionine. Incubation with [^{35}S]methionine/cysteine labels both proinsulins. Immunoprecipitation of the precursor and mature form showed a decrease in maturation of proinsulin II in the KO islets (Fig. 2*A*), as 29% of total protein was processed by KO islets compared with 46% in the WT condition. This difference was leveled out when both proinsulin I and II were labeled (data not shown). Conversion of the α cell secretory product, proglucagon to glucagon, seemed also to be disturbed in the furin-deficient islets (Fig. S2*A*), as 19% mature product was found compared with 28% mature glucagon in normal islets.

No difference in the processing of proPC1/3 to PC1/3 was found (Fig. 2*C*), whereas maturation of PC2 appeared affected in the furin-deficient islets (Fig. 2*B*). Under these conditions, only 25% of total PC2 was processed by KO islets, compared with 43% by WT islets.

CPE was processed to 67% in furin-deficient islets, compared with 77% in WT islets (Fig. S2*B*). A difference in the amount of processed 7B2 was observed also between WT (92%) and KO (79%) islets (Fig. S2*C*).

In conclusion, furin deficiency resulted in an indirect processing problem of known PC2 substrates (proPC2, proinsulin II, and proglucagon) (12, 21, 22). A direct effect of furin inactivation on the processing of its candidate substrates 7B2 and CPE was also noticed (15, 23).

Disturbed Intragranular Acidification in the Furin-Deficient β Cells. A common denominator for impaired secretion and reduced PC2 activity could be disturbed acidification of the dense-core secretory granules (DCSG) (17, 24). Therefore, acidification was analyzed by incubating mechanically dispersed islets with the acidotrophic agent DAMP. Insulin-positive cells were selected by using indirect immunofluorescence. Light intensity of the whole cell (with the exception of the nucleus), indirectly caused

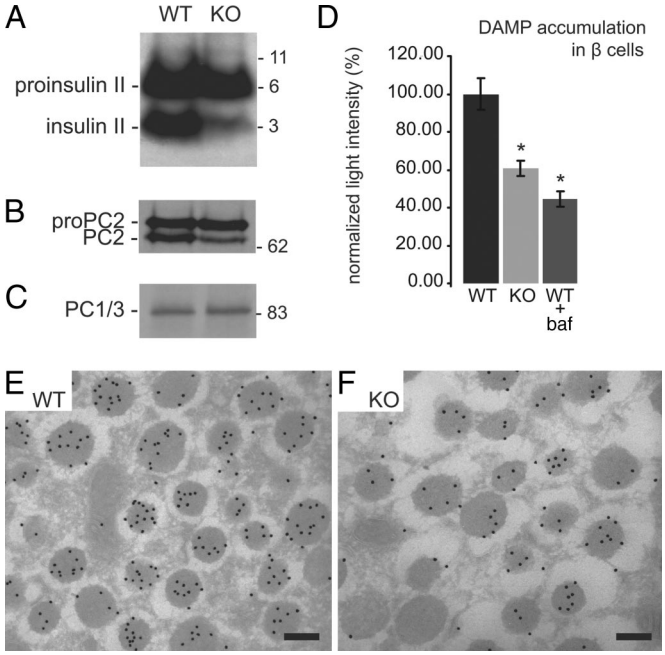

Fig. 2. Impaired processing of proproteins and disturbed intragranular acidification in the furin KO islets. (*A–C*) Isolated islets of both genotypes were radiolabeled (pulse, 0.5 h; chase, 1 h), and the lysates were immunoprecipitated with the appropriate antiserum. Insulin II (*A*), PC2 (*B*), and PC1/3 (*C*) are shown, and molecular masses are indicated (kDa). (*D*) Indirect immunofluorescence was performed on β cells, after 1 h of incubation with 30 μM DAMP (where appropriate cells were incubated with 100 nM baf). Mean light intensity per β cell was quantified. Average light intensity of WT β cells was set at 100%. Data represent means ± SEM. Two independent experiments were performed on a total of $n = 71$ WT β cells, $n = 103$ KO β cells, $n = 49$ WT β cells plus baf, isolated from six WT and four furin KO mice. *, $P < 0.05$. (*E* and *F*) Immunoelectron microscopy by using protein A conjugated to 15 nm of colloidal gold on cryosections of DAMP incubated islets. Scale bar, 200 nm. (*E*) β cell DCSG of a WT mouse containing an average of 6.7 particles per granule with $n = 685$ granules. (*F*) β cell DCSG of a KO mouse containing an average of 3.9 particles per granule with $n = 532$ granules.

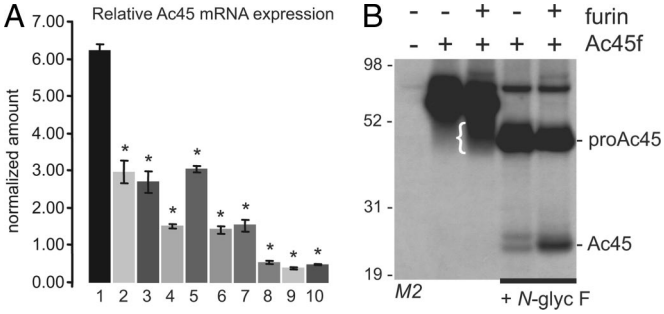

Fig. 3. V-ATPase accessory subunit Ac45 is abundant in islets of Langerhans and is *ex vivo* processed by furin. (*A*) Relative Ac45 mRNA expression in different tissues determined by quantitative reverse transcription PCR: 1, islets of Langerhans; 2, pancreatic acini; 3, pituitary gland; 4, adrenal gland; 5, lung; 6, brain; 7, bone marrow; 8, small intestine; 9, liver; 10, heart. The Ac45 expression of every sample was normalized to GAPDH and relative to the Ac45 expression in βTC3 cells, which was arbitrarily set at 1. Data represent mean ± SEM, $n = 3$. *, $P < 0.05$. (*B*) RPE.40 cells were transfected as indicated. (Co)transfection with empty pcDNA3 vector (−) was used as a negative control. Transfected RPE.40 cells were radiolabeled, and FLAG-tagged proteins were immunoprecipitated with M2 anti-FLAG antibody. Because of heterogeneity of glycosylation, the separation of glycosylated proAc45 and Ac45 by SDS/PAGE resulted in a smear (indicated with {). After deglycosylation with *N*-glycosidase F (*N*-glyc F; right two lanes), distinct protein bands were detected. The indicated positions of proAc45 and Ac45 correspond to the predicted Mw of the unglycosylated peptide backbone (46 and 24 kDa, respectively). Molecular masses are indicated (kDa).

by DAMP accumulation, was measured. The number of lysosomes in β cells is negligible compared with insulin granules (estimated as 48 and 11,000 per β cell, respectively; ref. 17) and, therefore, will not significantly contribute to the fluorescent signal. Furin KO β cells were significantly ($P = 3.5E\text{-}05$) reduced in light intensity to an average of 61% of the average light intensity of WT β cells (Fig. 2*D*). WT β cells incubated with the V-ATPase inhibitor bafilomycin A1 (baf) showed an even larger reduction in intensity (45%), as expected.

To demonstrate that the reduced intracellular accumulation of DAMP was the result of reduced acidification of DCSG, ImmunoGold electron microscopy was performed on DAMP-incubated islets (25) (Fig. 2 *E* and *F*). In WT islets an average of 6.7 Au particles per granule was found, compared with 3.9 Au particles per KO granule, which corresponds to a 42% reduction, similar to the results obtained with light microscopy. Only few gold particles were found in the cytosol, nuclei, and mitochondria (Fig. S3).

V-ATPase Accessory Subunit Ac45 Is Processed by Furin *ex Vivo*. Ac45, encoded by *Atp6ap1*, is a V-ATPase accessory subunit particularly abundant in neuroendocrine tissues (26, 27). Quantitative RT-PCR revealed highest expression of Ac45 in isolated islets of Langerhans as compared with nine other tissues (Fig. 3*A*, bar 1). Ac45 has been reported to be synthesized as a larger precursor (27). The bovine mature protein of 222 amino acids was found to start at Val-247, equivalent in mouse to a 219-aa mature protein starting at Ala-244. However, at 18 aa N-terminal of Val-247 (or Ala-244), there is a conserved PC consensus cleavage motif (RPSRVAR) (28, 29).

To study potential cleavage at this motif, recombinant mouse Ac45 was C-terminally labeled with a FLAG epitope tag. The furin-deficient CHO cell line, RPE.40 (30), was used to study the effect of proAc45f processing after reintroducing recombinant furin (Fig. 3*B*). Transfected cells were metabolically labeled and the FLAG-tagged proteins were immunoprecipitated. As described previously, mature Ac45 was observed as a broad smear at ≈45 kDa because of heterogeneity of glycosylation (26). Deglycosylation with *N*-glycosidase F converted the 62-kDa precursor into a 46-kDa band and mature Ac45 into a doublet of ≈24 kDa. Two faint protein bands were observed in the absence of furin. Cotransfection with furin led to an increase in the lower band of the doublet.

Because RXXR is known to be a furin consensus cleavage site and proAc45 contains RPSRVAR as a sequence, the exact cleavage site was further examined by inserting a FLAG tag at different positions (Fig. 4). Insertion of a FLAG tag C-terminally of a PC cleavage sequence is known not to interrupt existing furin cleavage (31), as the resulting P1′ Asp and P2′ Tyr are both favorable for furin. Immunoprecipitation with M1 antibody was performed as M1 only recognizes a FLAG epitope with a free N terminus. Only when the FLAG tag was positioned after Arg-225 (RRRf) was mature Ac45 visualized. Furthermore, substitution of the arginines by alanines resulted in blocked processing. Replacement of only Arg-219 by alanine did not affect processing (data not shown). The FLAG tag was also inserted at the previously described cleavage site (VfA), but no band was detected. In all experiments, expression was confirmed by immunoprecipitation with M2 antibody, which recognizes the FLAG tag independently of its position (Fig. 4*B Upper*).

***Ex Vivo* Knockdown of Furin and Ac45 Mimics the *in Vivo* Phenotype.** To investigate whether the phenotype of the furin-deficient islets could be mimicked in the mouse insulinoma βTC3 cell line, gene

CELL BIOLOGY

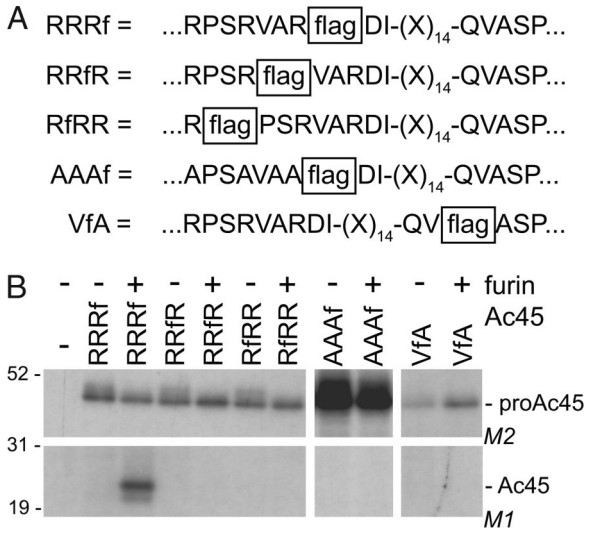

Fig. 4. Determination of the pro-Ac45 cleavage site. (*A*) Schematic representation of the different constructs. A FLAG epitope tag was inserted C-terminally of Arg-219 (RfRR), Arg-222 (RRfR), Arg-225 (RRRf), or Val-243 (VfA). RRRf was used as template to generate Ala-219-P-S-Ala-222-V-A-Ala-225-FLAG (AAAf). (*B*) RPE.40 cells were transfected with the different constructs in the presence or absence of a furin expression construct. (*Upper*) After radiolabeling, the lysates were divided in two, of which one half was immunoprecipitated with M2 antibody as a control for efficient expression of the construct. (*Lower*) Immunoprecipitation with M1 of cleaved Ac45 is shown. Results shown for the processing of AAAf are from an independent experiment. Molecular masses are indicated (kDa).

silencing experiments were performed. Short hairpin RNA (ShRNA) constructs for furin and Ac45 were designed and tested by cotransfection with the corresponding cDNA. Efficient silencing of exogenous furin in βTC3 cells has been described previously (32) and silencing of Ac45 is shown in Fig. 5*A*. Regulated secretion was analyzed by using recombinant FLAG-tagged Agouti-related protein (AGRPf) because it is a soluble protein, efficiently sorted to the regulated secretory pathway (32). Endogenous expression of furin and Ac45 in βTC3 cells was confirmed by reverse transcription PCR (data not shown). Knockdown of endogenous furin in βTC3 cells resulted in a significant 2.9-fold decrease in regulated secretion of AGRPf (Fig. 5*C*). Similarly, silencing of endogenous Ac45 led to a significant 3.4-fold reduction in regulated secretion.

Processing of recombinant proinsulin II was examined by cotransfecting the appropriate silencing construct with FLAG-tagged proinsulin II. Knockdown of furin nearly blocked proinsulin II processing in βTC3 cells (Fig. 5*B*). The same effect was observed again when endogenous Ac45 was depleted.

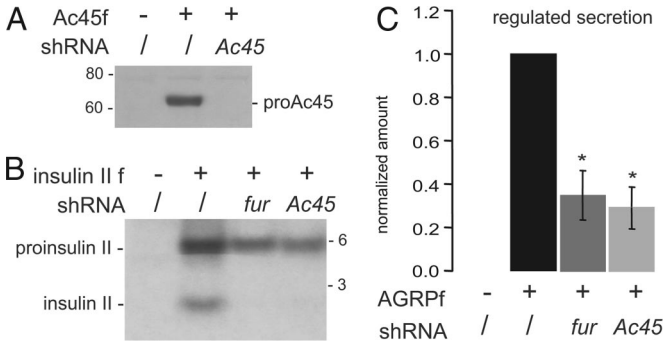

Fig. 5. Phenocopy obtained by gene silencing of *fur* or *Ac45* in βTC3 cells. (*A*) Efficacy of the shRNA against Ac45 was tested on the exogenous level of FLAG-tagged Ac45 (Ac45f) in βTC3 cells via Western blot analysis and detection with M2 anti-FLAG antibody. Molecular masses are indicated (kDa). (*B*) βTC3 cells were cotransfected with proinsulin II containing a C-terminal FLAG epitope and the empty mU6pro-vector (*/*), or the appropriate shRNA constructs. Cells were radiolabeled, and lysates were immunoprecipitated with M2 anti-FLAG antibody. Molecular masses are indicated (kDa). (*C*) βTC3 cells were cotransfected with a regulated secretion marker-protein AGRP-FLAG and the empty mU6pro-vector (*/*), or the appropriate shRNA constructs. Regulated secretion was defined as the amount of AGRPf secreted after stimulation with forskolin/IBMX minus tonic release and normalized for the total amount of AGRPf in lysates. Regulated secretion in the absence of any silencing constructs was arbitrarily set at 1. Data represent mean ± SEM, n = 4 for gene silencing of *fur*, n = 7 for gene silencing of *Ac45*. *, $P < 0.05$.

Discussion

The main physiological function of furin is assumed to be processing of substrates in the constitutive secretory pathway, in accordance with its accumulation in the TGN and expression in many cell types without regulated secretion. Our observations establish an important role for furin in the regulated secretory pathway. Impaired intragranular acidification significantly reduces secretion of insulin and slightly decreases processing of proinsulin II, proglucagon, and proPC2.

Proinsulin I contains a RQKR sequence at the C-A junction, whereas proinsulin II has a QQKR motif at this PC2 cleavage site. In PC2 null mice, PC1/3 is much more likely to compensate cleavage at the sequence motif containing an R at the P4 site than a Q in case of proinsulin II, resulting in a more severe processing problem of proinsulin II (21). Given the normal processing of PC1/3 in Fig. 2*C*, the decreased processing of proinsulin II is most likely caused by the low PC2 activity.

Because furin has been shown to cleave many proproteins *ex vivo*, it is possible that the impairments are the consequence of a compound phenotype. There are many reasons for proposing the accessory subunit of the V-ATPase Ac45 as the prime candidate to explain the observed phenotype. First, acidification is important for both aspects of the phenotype: regulated secretion and activity of PC2 (14, 17). Second, Ac45 is highly expressed in islets of Langerhans (Fig. 3*A*). Third, Ac45 mRNA is up-regulated tenfold in melanotrope cells of the *Xenopus* intermediate pituitary during black background adaptation, indicating a role in the regulated secretory pathway (33). Fourth, the yeast ortholog of furin, Kex2p, has been shown to have a role in the regulation of activity of the V-ATPase (19). Fifth, a KO mouse model for the *a*3 isoform of subunit *a* of the V-ATPase, which is highly expressed in the same neuroendocrine tissues as Ac45, also displays impaired exocytosis of insulin (34). Sixth, Ac45 contains a conserved furin cleavage site, which can be cleaved by furin *ex vivo* (Fig. 3*B*). Last, gene silencing of Ac45 in a β cell line resulted in a phenocopy, with reduced secretion and impaired proinsulin II processing (Fig. 5). Direct evidence for impaired processing *in vivo* could unfortunately not be obtained. Several attempts have been made to raise a specific antibody against Ac45. None of them were able to detect endogenous Ac45 in islets of Langerhans, possibly because of the highly hydrophobic nature of Ac45.

Determination of the exact cleavage site has ruled out the previously reported cleavage site, which was based on N-terminal sequencing of mature bovine Ac45 (27). Our results indicate proAc45 is cleaved by furin after Arg-225, possibly subsequently trimmed by aminopeptidase activity.

The effect of cleavage on its function cannot be unequivocally established, because the exact role of Ac45 in the V-ATPase is not yet known. However, gene silencing experiments (Fig. 5) suggest that the absence of Ac45 has the same effect as unprocessed Ac45. Therefore, processing of Ac45 appears to be a requirement for functionality. Given the relatively mild phenotype compared with the embryonic lethality of mice lacking the V-ATPase subunit *c* (PL16) (35), it is possible that processing is

not entirely blocked. Candidate PCs potentially providing redundancy are PACE4 and PC7, as both are expressed in the endocrine pancreas (36, 37). Another possibility is that Ac45 only modulates the function of V-ATPase activity. It has been demonstrated that the cytoplasmic tail of Ac45 might have a role in subcellular targeting of the V-ATPase (38). Alternatively, the membrane-integral section V_0 of V-ATPase has been shown to have a role in the terminal step of SNARE-mediated intracellular membrane fusion (39). Therefore, the transmembrane protein Ac45 may contribute to this membrane fusion event.

Impaired processing of several other proproteins might contribute to the phenotype as well. For example, pro7B2 has been suggested as a furin substrate and 7B2 is essential for PC2 activity (13, 15). The detection of decreased, but still clearly present, amounts of mature 7B2 establishes an at least partly redundant role for furin. Processing of proCPE was also investigated because of its role in proprotein maturation and regulated secretion (23, 40). However, furin inactivation disables only a small fraction of proCPE cleavage.

The presence of mislocalized α and δ cells within β cells suggests that furin has a role in the differentiation and/or maturation of β cells as well. Abnormal α/β cell topology has been described in GLP-1 receptor-deficient mice, for example (41). Until the furin target responsible is identified, we can only speculate about the responsible mechanism in our model.

The observed phenotype (impaired insulin secretion and processing) shows a similarity with early stages of type 2 diabetes. In certain idiopatic type 2 diabetic mouse models, misregulation of acidification has been shown to occur in the islets of Langerhans (42). To our knowledge, this is the first time a putative cause of acidification impairment resulting in a type 2 diabetes-like phenotype in mouse has been described. Therefore, Ac45 might be considered as a candidate gene for type 2 diabetes, although it is not located on any of the major susceptibility loci [Online Mendelian Inheritance of Man (OMIM) accession no. 125853].

Together, genetic ablation of furin in the endocrine pancreas results in disturbed intragranular acidification, with reduced secretion of insulin and slightly affected maturation of typical PC2 substrates as a consequence. We propose that impaired processing of Ac45, an accessory subunit of the V-ATPase, is the main cause of the observed acidification problem. The molecular mechanism showing how Ac45 affects V-ATPase function in secretory granules remains to be studied.

Materials and Methods

***Fur*$^{flox/flox}$ *Pdx1-Cre* Mice.** The previously described B6J/129 *fur*$^{flox/flox}$ mice (6) were crossed with B6J/CBAJ *Pdx1-Cre* transgenic mice (20). Genotyping was performed with reported primers (6, 20). Confirming deletion of the floxed *fur* exon 2 is described in *SI Materials and Methods*.

All procedures were conducted according to protocols and guidelines approved by the Katholieke Universiteit Leuven animal welfare committee.

Glucose Tolerance Test. See *SI Materials and Methods* for information.

Isolation of Mouse Pancreatic Islets. Islets of Langerhans were isolated as described (43, 44).

Measurement of Insulin Content and Release. Insulin release was measured by using perifusion experiments in a multiple microchamber module as described previously (44).

Immunofluorescence. Islets were mechanically dissociated as described (17) to obtain separate β cells after incubation of the islets for 10 min at 37°C in a Ca^{2+}-free solution (138 mM NaCl/5.6 mM KCl/1.2 mM $MgCl_2$/5 mM HEPES/1 mM EGTA/1 mg/ml BSA/3 mM glucose). Cells were adhered on polylysine-coated glass slides for 1 h, followed by a 1-h preincubation in Hanks' balanced salt solution (1.67 mM glucose) with or without 100 nM baf (Sigma). 30 μM DAMP (Molecular Probes) was subsequently added to the medium for 1 h. Method of indirect immunofluorescence is given in *SI Materials and Methods*. Anti-DNP (Molecular Probes; 1:10,000) was used to detect DAMP, anti-insulin (as described below; 1:2,500) to select for β cells. Secondary antibodies were Alexa Fluor 594 and 488 (Molecular Probes). Analysis of the slides and quantification of light intensity are described in *SI Materials and Methods*.

Immunoelectron Microscopy. Detailed description of the applied method is available in *SI Materials and Methods*. Briefly, isolated islets were fixed with 4% formaldehyde/0.1% glutaraldehyde in 0.1 M sodium cacodylate buffer. Ultrathin cryosections were generated (45) and mounted on formvar-carbon coated EM grids. Anti-DNP antibody (1:100) was detected with protein A conjugated to 15 nm colloidal gold. The sections were contrasted by embedding in 1.8% methyl cellulose, containing 0.3% uranyl acetate and observed in a Philips CM100 transmission electron microscope at an operating voltage of 80 kV.

We collected and recorded 50 micrographs of each condition by using a MegaView III CCD camera and iTEM software (Olympus). We circumscribed 685 WT granules and 532 KO granules by using the software to record the number of gold particles labeling each granule.

Quantitative RT-PCR. Details on RNA extraction and Quantitative PCRs are provided in *SI Materials and Methods*.

Constructs. A cDNA construct containing full-length mouse Ac45 was kindly provided by G. J. Martens, Nijmegen (46) and subcloned in pcDNA3 (Invitrogen). A FLAG epitope tag (DYKDDDDK) was inserted C-terminally of Arg-219 (RfRR), Arg-222 (RRfR), Arg-225 (RRRf), Val-243 (VfA), or Val-463 (Ac45f) by using a Quick-Change site-directed mutagenesis kit (Stratagene) by following manufacturer's protocols. RRRf was used as a template to generate Ala-219-P-S-Ala-222-V-A-Ala-225-FLAG (AAAf). Insulin II was PCR amplified from βTC3 cDNA, and a FLAG tag was inserted C-terminally (Asn-110). All constructs were analyzed by nucleotide sequencing.

The expression constructs of furin (8) and AGRP-FLAG (32) were used as described.

RNA Interference. Description of the shRNA constructs used is given in *SI Materials and Methods*.

Cell Lines and Transfections. See *SI Materials and Methods* for information on cell lines and transfections.

Radiolabeling and Immunoprecipitation. Isolated islets were radiolabeled and immunoprecipitated as described (47) by using insulin monoclonal antibody 3B7 (provided by J. C. Hutton, Denver) (48), PC1/3 antiserum, and PC2 antiserum (both Alexis Biochemicals).

Transfected cell lines were preincubated in methionine/cysteine-free RPMI medium 1640 (Sigma) for 1 h at 37°C and then labeled in the same medium containing 100 μCi [^{35}S]methionine/cysteine (1 Ci = 37 GBq; Easytag express protein labeling mixture, PerkinElmer; specific activity, 1,175 Ci/mmol) for another hour. Cells were then chased in medium containing excess (0.4 mM) unlabeled methionine and cysteine for 2 h at 37°C (1 h 30 min for proinsulin II immunoprecipitation). Cell lysates were precleared by using mouse serum (GE Healthcare). Immunoprecipitation was performed (2 h, 4°C) by using anti-FLAG antibodies M1 or M2 (Sigma) bound to protein G Sepharose. After washing, immune complexes were directly eluted from the Sepharose by using sample buffer in case of proinsulin processing analysis. In case of Ac45 processing experiments, proteins bound to Sepharose were deglycosylated overnight at 37°C. Proteins were then eluted by adding NuPage LDS sample buffer and reducing agent (both Invitrogen) and analyzed by SDS/PAGE (Criterion, Bio-Rad; NuPage, Invitrogen). Autoradiographic signals were obtained after fixing (30% methanol/10% acetic acid) and incubating in NAMP100V (GE Healthcare). Detailed information is described in *SI Materials and Methods*.

Regulated Secretion Assay. Regulated secretion experiments were performed essentially as described (8), except that cells were incubated overnight in nonsupplemented serum-free DMEM. Sample preparation and separation by SDS/PAGE have been described previously (32). For Western blotting (49), anti-FLAG antibody M2 (Sigma) was used. The chemiluminescent signal was quantified by using Kodak Digital Science (Kodak Imager with 1D Image Analysis software, version 3.0). Detailed calculations of regulated secretion are specified in *SI Materials and Methods*.

Statistical Analysis. Results are expressed as means ± SEM. Except for the regulated secretion assay, statistical analysis was performed by the unpaired Student's *t* test, where $P < 0.05$ was considered significant. For each of the two groups of regulated secretion data separately, a one-sample *t* test (H0: $\mu = 1$ and

two-sided P value) has been used to verify the difference ($P < 0.05$) with the control.

ACKNOWLEDGMENTS. We thank I. Pauli and J. Laureys for excellent technical assistance. This work was supported by the Instituut voor de Aanmoeding van Innovatie door Wetenschap en Technologie in Vlaanderen (IWT), the Fonds voor Wetenschappelijk Onderzoek Vlaanderen (FWO Vlaanderen), and the Geconcerteerde Onderzoeksactie van de Vlaamse Gemeenschap (GOA 2008/16 and GOA 2004/11). N.A.B. was supported by the Medical Research Council (London, United Kingdom).

1. Taylor NA, Van de Ven WJ, Creemers JW (2003) Curbing activation: proprotein convertases in homeostasis and pathology. *FASEB J* 17:1215–1227.
2. Seidah NG, Prat A (2002) Precursor convertases in the secretory pathway, cytosol and extracellular milieu. *Essays Biochem* 38:79–94.
3. Steiner DF (1998) The proprotein convertases. *Curr Opin Chem Biol* 2:31–39.
4. Scamuffa N, Calvo F, Chretien M, Seidah NG, Khatib AM (2006) Proprotein convertases: lessons from knockouts. *FASEB J* 20:1954–1963.
5. Roebroek AJ, *et al.* (1998) Failure of ventral closure and axial rotation in embryos lacking the proprotein convertase Furin. *Development* 125:4863–4876.
6. Roebroek AJ, *et al.* (2004) Limited redundancy of the proprotein convertase furin in mouse liver. *J Biol Chem* 279:53442–53450.
7. Kayo T, *et al.* (1997) Proprotein-processing endoprotease furin controls growth of pancreatic beta-cells. *Diabetes* 46:1296–1304.
8. Creemers JW, *et al.* (1996) Identification of a transferable sorting domain for the regulated pathway in the prohormone convertase PC2. *J Biol Chem* 271:25284–25291.
9. Dittie AS, Thomas L, Thomas G, Tooze SA (1997) Interaction of furin in immature secretory granules from neuroendocrine cells with the AP-1 adaptor complex is modulated by casein kinase II phosphorylation. *EMBO J* 16:4859–4870.
10. Goodge KA, Hutton JC (2000) Translational regulation of proinsulin biosynthesis and proinsulin conversion in the pancreatic beta-cell. *Semin Cell Biol* 11:235–242.
11. Davidson HW, Hutton JC (1987) The insulin-secretory-granule carboxypeptidase H. Purification and demonstration of involvement in proinsulin processing. *Biochem J* 245:575–582.
12. Muller L, Lindberg I (1999) The cell biology of the prohormone convertases PC1 and PC2. *Prog Nucleic Acid Res Mol Biol* 63:69–108.
13. Mbikay M, Seidah NG, Chretien M (2001) Neuroendocrine secretory protein 7B2: structure, expression and functions. *Biochem J* 357:329–342.
14. Lamango NS, Apletalina E, Liu J, Lindberg I (1999) The proteolytic maturation of prohormone convertase 2 (PC2) is a pH-driven process. *Arch Biochem Biophys* 362:275–282.
15. Paquet L, *et al.* (1994) The neuroendocrine precursor 7B2 is a sulfated protein proteolytically processed by a ubiquitous furin-like convertase. *J Biol Chem* 269:19279–19285.
16. Davidson HW, Rhodes CJ, Hutton JC (1988) Intraorganellar calcium and pH control proinsulin cleavage in the pancreatic beta cell via two distinct site-specific endopeptidases. *Nature* 333:93–96.
17. Barg S, *et al.* (2001) Priming of insulin granules for exocytosis by granular Cl(-) uptake and acidification. *J Cell Sci* 114:2145–2154.
18. Schoonderwoert VT, Martens GJ (2001) Proton pumping in the secretory pathway. *J Membr Biol* 182:159–169.
19. Oluwatosin YE, Kane PM (1998) Mutations in the yeast KEX2 gene cause a Vma(-)-like phenotype: a possible role for the Kex2 endoprotease in vacuolar acidification. *Mol Cell Biol* 18:1534–1543.
20. Herrera PL (2000) Adult insulin- and glucagon-producing cells differentiate from two independent cell lineages. *Development* 127:2317–2322.
21. Furuta M, *et al.* (1998) Incomplete processing of proinsulin to insulin accompanied by elevation of Des-31,32 proinsulin intermediates in islets of mice lacking active PC2. *J Biol Chem* 273:3431–3437.
22. Rouille Y, Westermark G, Martin SK, Steiner DF (1994) Proglucagon is processed to glucagon by prohormone convertase PC2 in alpha TC1–6 cells. *Proc Natl Acad Sci USA* 91:3242–3246.
23. Song L, Fricker L (1995) Processing of procarboxypeptidase E into carboxypeptidase E occurs in secretory vesicles. *J Neurochem* 65:444–453.
24. Schoonderwoert VT, Holthuis JC, Tanaka S, Tooze SA, Martens GJ (2000) Inhibition of the vacuolar H+-ATPase perturbs the transport, sorting, processing and release of regulated secretory proteins. *Eur J Biochem* 267:5646–5654.
25. Orci L, *et al.* (1986) Conversion of proinsulin to insulin occurs coordinately with acidification of maturing secretory vesicles. *J Cell Biol* 103:2273–2281.
26. Supek F, *et al.* (1994) A novel accessory subunit for vacuolar H(+)-ATPase from chromaffin granules. *J Biol Chem* 269:24102–24106.
27. Getlawi F, *et al.* (1996) Chromaffin granule membrane glycoprotein IV is identical with Ac45, a membrane-integral subunit of the granule's H(+)-ATPase. *Neurosci Lett* 219:13–16.
28. Henrich S, *et al.* (2003) The crystal structure of the proprotein processing proteinase furin explains its stringent specificity. *Nat Struct Biol* 10:520–526.
29. Rockwell NC, Krysan DJ, Komiyama T, Fuller RS (2002) Precursor processing by kex2/furin proteases. *Chem Rev (Washington, DC)* 102:4525–4548.
30. Moehring JM, Inocencio NM, Robertson BJ, Moehring TJ (1993) Expression of mouse furin in a Chinese hamster cell resistant to Pseudomonas exotoxin A and viruses complements the genetic lesion. *J Biol Chem* 268:2590–2594.
31. Molloy SS, Thomas L, VanSlyke JK, Stenberg PE, Thomas G (1994) Intracellular trafficking and activation of the furin proprotein convertase: localization to the TGN and recycling from the cell surface. *EMBO J* 13:18–33.
32. Creemers JW, *et al.* (2006) Agouti-related protein is posttranslationally cleaved by proprotein convertase 1 to generate agouti-related protein (AGRP)83–132: interaction between AGRP83–132 and melanocortin receptors cannot be influenced by syndecan-3. *Endocrinology* 147:1621–1631.
33. Holthuis JC, Jansen EJ, van Riel MC, Martens GJ (1995) Molecular probing of the secretory pathway in peptide hormone-producing cells. *J Cell Sci* 108 (Pt 10):3295–3305.
34. Sun-Wada GH, *et al.* (2006) The a3 isoform of V-ATPase regulates insulin secretion from pancreatic beta-cells. *J Cell Sci* 119:4531–4540.
35. Sun-Wada G, *et al.* (2000) Acidic endomembrane organelles are required for mouse postimplantation development. *Dev Biol* 228:315–325.
36. Nagamune H, *et al.* (1995) Distribution of the Kexin family proteases in pancreatic islets: PACE4C is specifically expressed in B cells of pancreatic islets. *Endocrinology* 136:357–360.
37. Seidah NG, *et al.* (1996) cDNA structure, tissue distribution, and chromosomal localization of rat PC7, a novel mammalian proprotein convertase closest to yeast kexin-like proteinases. *Proc Natl Acad Sci USA* 93:3388–3393.
38. Jansen EJ, Holthuis JC, McGrouther C, Burbach JP, Martens GJ (1998) Intracellular trafficking of the vacuolar H+-ATPase accessory subunit Ac45. *J Cell Sci* 111(Pt 20):2999–3006.
39. Peters C, *et al.* (2001) Trans-complex formation by proteolipid channels in the terminal phase of membrane fusion. *Nature* 409:581–588.
40. Cool DR, *et al.* (1997) Carboxypeptidase E is a regulated secretory pathway sorting receptor: genetic obliteration leads to endocrine disorders in Cpe(fat) mice. *Cell* 88:73–83.
41. Ling Z, *et al.* (2001) Glucagon-like peptide 1 receptor signaling influences topography of islet cells in mice. *Virchows Arch* 438:382–387.
42. Gunawardana SC, Head WS, Piston DW (2005) Amiloride derivatives enhance insulin release in pancreatic islets from diabetic mice. *BMC Endocr Disord* 5:9.
43. Boonen K, *et al.* (2007) Neuropeptides of the islets of Langerhans: a peptidomics study. *Gen Comp Endocrinol* 152:231–241.
44. Flamez D, *et al.* (1998) Mouse pancreatic beta-cells exhibit preserved glucose competence after disruption of the glucagon-like peptide-1 receptor gene. *Diabetes* 47:646–652.
45. Liou W, Geuze HJ, Slot JW (1996) Improving structural integrity of cryosections for immunogold labeling. *Histochem Cell Biol* 106:41–58.
46. Schoonderwoert VT, Martens GJ (2002) Structural gene organization and evolutionary aspects of the V-ATPase accessory subunit Ac45. *Biochim Biophys Acta* 1574:245–254.
47. Scheuner D, *et al.* (2005) Control of mRNA translation preserves endoplasmic reticulum function in beta cells and maintains glucose homeostasis. *Nat Med* 11:757–764.
48. Grimaldi KA, Hutton JC, Siddle K (1987) Production and characterization of monoclonal antibodies to insulin secretory granule membranes. *Biochem J* 245:557–566.
49. Creemers JW, van de Loo JW, Plets E, Hendershot LM, Van de Ven WJ (2000) Binding of BiP to the processing enzyme lymphoma proprotein convertase prevents aggregation, but slows down maturation. *J Biol Chem* 275:38842–38847.